Liquid Crystals
Publication details, including instructions for authors and subscription information:
http://www.informaworld.com/smpp/title~content=t713926090

Synthesis and characterization of new series of ferroelectric liquid crystals containing oligooxyethylene spacers

Jr-Hong Chen[a]; Rong-Chi Chang[a]; Ging-Ho Hsiue[a]; Feng-Wei Guu[a]; Shung-Long Wu[b]
[a] Department of Chemical Engineering, National Tsing Hua University, Hsinchu, Taiwan, Republic of China [b] Department of Chemical Engineering, Tatung Institute of Technology, Taipei, Taiwan, Republic of China

To cite this Article Chen, Jr-Hong , Chang, Rong-Chi , Hsiue, Ging-Ho , Guu, Feng-Wei and Wu, Shung-Long(1995) 'Synthesis and characterization of new series of ferroelectric liquid crystals containing oligooxyethylene spacers', Liquid Crystals, 18: 2, 291 — 301
To link to this Article: DOI: 10.1080/02678299508036625
URL: http://dx.doi.org/10.1080/02678299508036625

LIQUID CRYSTALS, 1995, VOL. 18, NO. 2, 291–301

Synthesis and characterization of new series of ferroelectric liquid crystals containing oligooxyethylene spacers

by JR-HONG CHEN, RONG-CHI CHANG, GING-HO HSIUE*
and FENG-WEI GUU

Department of Chemical Engineering, National Tsing Hua University, Hsinchu, Taiwan, Republic of China

and SHUNG-LONG WU

Department of Chemical Engineering, Tatung Institute of Technology, Taipei 10451, Taiwan, Republic of China

(*Received 21 April 1994; accepted 15 May 1994*)

Four series of ferroelectric liquid crystals containing oligooxyethylene spacers have been synthesized. These obtained liquid crystal compounds were characterized by NMR, differential scanning calorimetry (DSC) and optical polarized microscopy (POM). The properties of the liquid crystalline phase were investigated as a function of spacer units, numbers of core aromatic rings, and different terminal asymmetric moieties. It was found that (i) the phase transition temperature decreased with the increasing oligooxyethylene spacer unit, (ii) the liquid crystalline phases were enhanced in three phenyl ring system than in two phenyl ring system, and (iii) ferroelectric liquid crystals containing different terminal asymmetric moieties exhibited novel mesophase phenomena. A twist grain boundary phase (TGB_A phase) was observed in some compounds of this study. Furthermore, a wide temperature chiral smectic C range including room temperature was achieved.

1. Introduction

The first ferroelectric liquid crystal (FLC) was discovered in 1975 by Meyer *et al.* [1]. Prompted by the development of the surface stabilized ferroelectric liquid crystal display technology [2], the physics and technology of the FLC cell have been extensively developed [3–6]. Thus, great advances have been made toward the realization and application of practical devices [7, 8].

It is desirable for a FLC display that the ferroelectric liquid crystal material shows a smectic phase over a wide range of temperatures including room temperature [9]. Furthermore, a large spontaneous polarization is required. A FLC related device can be operated at a reduced driving voltage as a result. These properties are influenced by the molecular structures of liquid crystal compounds. Consequently, it is of interest to synthesize ferroelectric liquid crystal compounds and compositions which exhibit favorable spontaneous polarization values and exhibit smectic character over a wide range of temperatures, especially at room temperature.

Besides low molar mass FLCs, several side-chain liquid crystalline polymers (LCPs) exhibiting a chiral smectic C mesophase have been reported [10–13]. Ferroelectric properties, for example, spontaneous polarization in these polymers, have also been provided in some cases [10–13]. As a part of the research program dedicated to the development of high efficiency FLC materials, we have designed and synthesized some novel low molar mass FLCs and ferroelectric side-chain liquid crystalline polymers [14, 15]. They exhibit a broad temperature range chiral smectic C phase and satisfactory electro-optical properties [15].

In this paper, we have synthesized and characterized four series of ferroelectric liquid crystals. These materials contained oligooxyethylene spacers, various chiral moieties, and two or three aromatic rings of ester core units. The influence of the spacer unit and different chiral tails on formation of mesophases is discussed.

The new series have the general formulae:

Series I

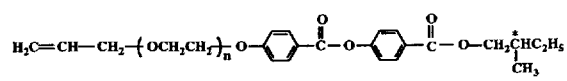

$n = 0, 1, 2, 3$ (MDn11A)

* Author for correspondence.

0267–8292/95 $10·00

Series II

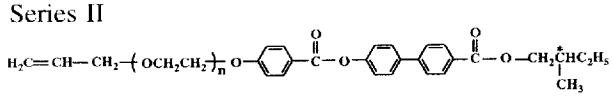

$n = 0, 1, 2, 3$ (MDn12A)

Series III

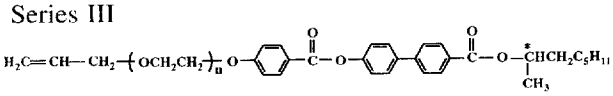

$n = 0, 1, 2, 3$ (MDn12B)

Series IV

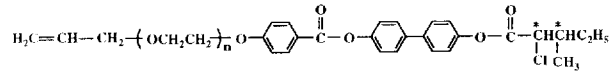

$n = 0, 1, 2, 3$ (MDn12C)

2. Synthesis

The compounds of series MDn11A, MDn12A, MDn12B and MDn12C were prepared following the schemes 1 and 2.

Synthetic details of the above reactions are described in the experimental section.

3. Results and discussion

The phase sequences and the corresponding transition temperatures for these new series are reported in table 1 (*a*), (*b*), and figure 1 (*a*), (*b*), (*c*).

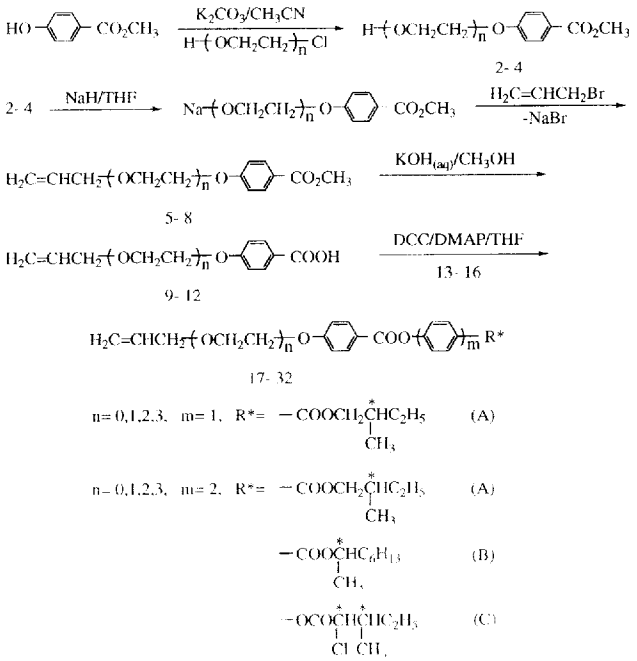

THF: tetrahydrofuran; DCC: *N*,*N*′-dicyclohexyl carbodiimide; DMAP: 4-(dimethyl amino) pyridine.

Scheme 1. Synthesis of series MDn11A, MDn12A, MDn12B, and MDn12C.

3.1. *Optical microscopy*

3.1.1. *Series MDn11A*

The series were composed of two phenyl rings interconnected via a single ester linkage and (*S*)-2-methyl-1-butyl chiral tail groups. However, these compounds exhibited few mesomorphic phases and no chiral smectic C phase. Only the derivative with a short spacer chain ($n = 0$) showed smectic A phase. Other ordered smectic phases were present in MD011A, and MD111A, MD211A and MD311A were viscous liquids and were not liquid crystalline.

3.1.2. *Series MDn12A*

The four members of this series contained an (*S*)-2-methyl-1-butyl chiral moiety and oxyethylene unit chains, in addition to a biphenyl ring within the mesogen core. The biphenyl ring in the mesogen core revealed richer mesomorphic behaviour compared to the series MDn11A (see figure 1 (*a*)). Series MDn12A were all enantiotropic. The first derivative which has no oxyethylene unit ($n = 0$) exhibited a blue phase (BP), the cholesteric (Ch) phase, and the classical smectic A phase with focal-conic or homeotropic texture. The other three derivatives ($n = 1$–3) displayed a blue phase–cholesteric–twist grain boundary A phase–smectic A–chiral smectic C (BP–Ch–TGB$_A$–S$_A$–S$_C^*$) liquid crystal sequence. The transition from the isotropic liquid to blue phase II (BPII) (between two untreated glass plates) was somewhat difficult to be observed by POM, but easily detected by calorimetric studies. A grazed platelet texture could be observed clearly at the transition from BPII to blue phase I (BPI). Upon cooling, scale-like and paramorphotic defective textures grew gradually during

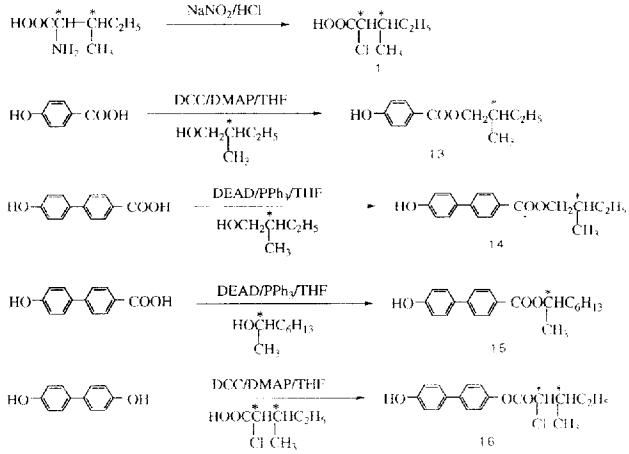

DEAD: diethyl azodicarboxylate; PPh$_3$: triphenyl phosphine; THF: tetrahydrofuran; DCC: *N*,*N*′-dicyclohexyl carbodiimide; DMAP: 4-(dimethyl amino)-pyridine.

Scheme 2. Synthesis of chiral compounds **1**, and **13**–**16**.

Table 1. (*a*) Transition temperatures for the MDn11A and MDn12A series.

Name	*n*	Phase transition °C (corresponding enthalpy changes, mJ mg^{-1}) $\left[\frac{\text{Heating}}{\text{Cooling}}\right]$
MD011A	0	$\frac{\text{C}\ 48{\cdot}52(-)\ \text{S}_\text{A}\ 50{\cdot}92(55)\dagger\ \text{I}}{\text{I}\ 25(-)\ \text{S}_\text{A}\ 21{\cdot}65(-)\ \text{S}\ 18{\cdot}84(62{\cdot}1)\ddagger\ \text{C}}$
MD111A	1	$\frac{\text{C}\ 16{\cdot}62(2{\cdot}6)\ \text{S}\ 38{\cdot}43(50{\cdot}7)\ \text{I}}{\text{I}\ 23{\cdot}09(51{\cdot}5)\ \text{S}\ 15{\cdot}5(2{\cdot}0)\ \text{C}}$
MD211A	2	$\frac{\text{C–§I}}{\text{I–§C}}$
MD311A	3	$\frac{\text{C–§I}}{\text{I–§C}}$
MD012A	0	$\frac{\text{C}\ 97{\cdot}8(58{\cdot}65)\ \text{S}_\text{A}\ 144(2{\cdot}58)\ \text{Ch}\ 180(1{\cdot}3)\ \text{I}}{\text{I}\ 180\ \text{BP}\ 178(1{\cdot}3)\ \text{Ch}\ 136(2{\cdot}6)\ \text{S}_\text{A}\ 54{\cdot}4(45{\cdot}16)\ \text{C}}$
MD112A	1	$\frac{\text{C}\ 71{\cdot}4(39{\cdot}1)\ \text{S}_\text{C}^*\ 95(0{\cdot}6)\ \text{S}_\text{A}\ 127{\cdot}2(1{\cdot}6)\ \text{Ch}\ 145{\cdot}1(1{\cdot}0)\ \text{I}}{\text{I}\ 151{\cdot}9\ \text{BP}\ 144(0{\cdot}9)\|\ \text{Ch}\ 126{\cdot}6(1{\cdot}2)\P\ \text{TGB}_\text{A}\ 125{\cdot}7(-)\ \text{S}_\text{A}\ 93(0{\cdot}8)\ \text{S}_\text{C}^*\ 1{\cdot}5(20)\ \text{C}}$
MD212A	2	$\frac{\text{C}\ 62{\cdot}4(61{\cdot}6)\ \text{S}_\text{C}^*\ 79(0{\cdot}9)\ \text{S}_\text{A}\ 93{\cdot}5(2{\cdot}3)\ \text{Ch}\ 107{\cdot}5(1{\cdot}1)\ \text{I}}{\text{I}\ 108{\cdot}4\ \text{BPII}\ 106{\cdot}3\ \text{BPI}\ 106(0{\cdot}9)\dagger\dagger\ \text{Ch}\ 94{\cdot}9(2{\cdot}0)\P\ \text{TGB}_\text{A}\ 93{\cdot}3(-)\ \text{S}_\text{A}\ 78(1{\cdot}0)\ \text{S}_\text{C}^*\ -\ 8{\cdot}5(16{\cdot}8)\ \text{C}}$
MD312A	3	$\frac{\text{C}\ 19{\cdot}5(-)\ \text{S}_\text{C}^*\ 49{\cdot}5(0{\cdot}6)\ \text{S}_\text{A}\ 57{\cdot}4(1{\cdot}2)\ \text{Ch}\ 71{\cdot}4(0{\cdot}7)\ \text{I}}{\text{I}\ 69\ \text{BPII}\ 67{\cdot}3\ \text{BPI}\ 60{\cdot}5(0{\cdot}6)\dagger\dagger\ \text{Ch}\ 55(1{\cdot}2)\|\ \text{TGB}_\text{A}\ 51{\cdot}2(-)\ \text{S}_\text{A}\ 49(1{\cdot}1)\ \text{S}_\text{C}^*\ -\ 42{\cdot}3(-)\ddagger\ddagger\ \text{C}}$

† $\Delta\underline{\text{H}}$(C–$\text{S}_\text{A}$–I). ‡ $\Delta\underline{\text{H}}$(I–$\text{S}_\text{A}$–S–K). § No liquid crystalline phase was observed and melting point was below −20°C. ‖ $\Delta\underline{\text{H}}$(I–BP–Ch). ¶ $\Delta\underline{\text{H}}$(Ch–$\text{TGB}_\text{A}$–$\text{S}_\text{A}$). †† $\Delta\underline{\text{H}}$(I–BPII–BPI–Ch). ‡‡ Enthalpies were too small to be evaluated.

Table 1. (*b*) Transition temperatures for the MDn12B and MDn12C series.

Name	*n*	Phase transition °C (corresponding enthalpy changes, mJ mg^{-1}) $\left[\frac{\text{Heating}}{\text{Cooling}}\right]$
MD012B	0	$\frac{\text{C}\ 84{\cdot}7(42{\cdot}3)\ \text{S}_\text{A}\ 136{\cdot}9(10{\cdot}3)\ \text{I}}{\text{I}\ 133{\cdot}3(10{\cdot}1)\ \text{S}_\text{A}\ 33{\cdot}51\ (19{\cdot}3)\ \text{C}}$
MD112B	1	$\frac{\text{C}\ 65{\cdot}5(39{\cdot}2)\dagger\ \text{S}_\text{C}^*\ 69{\cdot}1(-)\ \text{S}_\text{A}\ 104{\cdot}1(5{\cdot}5)\ \text{I}}{\text{I}\ 101{\cdot}9(5{\cdot}65)\ \text{S}_\text{A}\ 27{\cdot}5(-)\ \text{S}_\text{C}^*\ 24{\cdot}3(22{\cdot}6)\dagger\ \text{C}}$
MD212B	2	$\frac{\text{C}\ 72{\cdot}54(54{\cdot}04)\ \text{I}}{\text{I}\ 58{\cdot}4(4{\cdot}94)\ \text{S}_\text{A}\ 28(37{\cdot}3)\ \text{S}_\text{C}^*\ 26{\cdot}7\ \text{C}}$
MD312B	3	$\frac{\text{C}\ -\ 40(0{\cdot}6)\ \text{S}_1\ -\ 14{\cdot}11(0{\cdot}2)\ \text{S}_2\ -\ 7{\cdot}14(0{\cdot}3)\ \text{S}_3\ 19{\cdot}72(3{\cdot}8)\ \text{I}}{\text{I}\ 20{\cdot}8(-)\ \text{S}_\text{A}\ 16{\cdot}48(4{\cdot}0)\ddagger\ \text{S}_3\ -\ 4{\cdot}7(0{\cdot}4)\ \text{S}_2\ -\ 12{\cdot}76(0{\cdot}2)\ \text{S}_1\ -\ 46{\cdot}05(-)\S\ \text{C}}$
MD012C	0	$\frac{\text{C}\ 78{\cdot}9(19{\cdot}8)\ \text{S}_\text{A}\ 100(1{\cdot}0)\ \text{Ch}\ 181{\cdot}7(0{\cdot}8)\ \text{I}}{\text{I}\ 179{\cdot}5\ \text{BP}\ 178(1{\cdot}4)\ \text{Ch}\ 92{\cdot}3(1{\cdot}2)\|\ \text{TGB}_\text{A}\ 84{\cdot}3(-)\ \text{S}_\text{A}\ 67{\cdot}5(15{\cdot}8)\ \text{C}}$
MD112C	1	$\frac{\text{C}\ 29{\cdot}9(7{\cdot}4)\ \text{S}\ 57{\cdot}1(1{\cdot}4)\ \text{S}_\text{C}^*\ 113{\cdot}2(7{\cdot}2)\ \text{Ch}\ 141{\cdot}7(0{\cdot}9)\ \text{I}}{\text{I}\ 142{\cdot}2\ \text{BPII}\ 141{\cdot}8\ \text{BPI}\ 136(1{\cdot}1)\ \text{Ch}\ 112{\cdot}1(7{\cdot}3)\ \text{S}_\text{C}^*\ 53{\cdot}9(1{\cdot}9)\ \text{S}\ 23{\cdot}9(1{\cdot}0)\ \text{C}}$
MD212C	2	$\frac{\text{C}\ -\ 9{\cdot}2(4{\cdot}2)\ \text{S}_\text{C}^*\ 88{\cdot}3(7{\cdot}3)\ \text{Ch}\ 103{\cdot}5(0{\cdot}8)\ \text{I}}{\text{I}\ 102\ \text{BPII}\ 96{\cdot}6\ \text{BPI}\ 90{\cdot}2(1{\cdot}8)\ \text{Ch}\ 85{\cdot}9(7{\cdot}8)\ \text{S}_\text{C}^*\ -\ 13{\cdot}9(5{\cdot}8)\ \text{C}}$
MD312C	3	$\frac{\text{C}\ -\ 25{\cdot}26(-)\S\ \text{S}_\text{C}^*\ 57{\cdot}59(5{\cdot}3)\ \text{BP}\ 63{\cdot}5(0{\cdot}2)\ \text{I}}{\text{I}\ 63{\cdot}77(0{\cdot}3)\ \text{BP}\ 58{\cdot}6(5{\cdot}3)\ \text{S}_\text{C}^*\ -\ 28{\cdot}13(-)\S\ \text{C}}$

† $\Delta\underline{\text{H}}$(C–$\text{S}_\text{C}^*$–$\text{S}_\text{A}$). ‡ $\Delta\underline{\text{H}}$(I–$\text{S}_\text{A}$–$\text{S}_3$). § Enthalpies were too small to be evaluated. ‖ ΔH(Ch–TGB_A–S_A).

the formation of the cholesteric phase [16]. Further cooling from the scale-like cholesteric phase, the TGB_A phase appeared as evidenced by the formation of filament textures [17–20] or Grandjean iridescent textures [21] (see figure 2 (*a*)). The textures were confirmed by the observation of pitch bands which are perpendicular to the long axes of the filaments. Below the transition temperature of TGB_A phase, a novel liquid crystalline behaviour of a smectic A phase was observed. The molecules apparently formed a smectic A phase through distortion of the helix of the TGB_A phase. However, the helical layer ordering of TGB_A phase did not completely unwind, instead, it remained in smectic A phase to form a novel spiral texture (see figure 2 (*b*)). The ferroelectric S_C^* phase cooling down the smectic A phase showed the striated lines of the fan domains. However, the spiral fan style of smectic A phase textures remained unchanged (see figure 2 (*c*)).

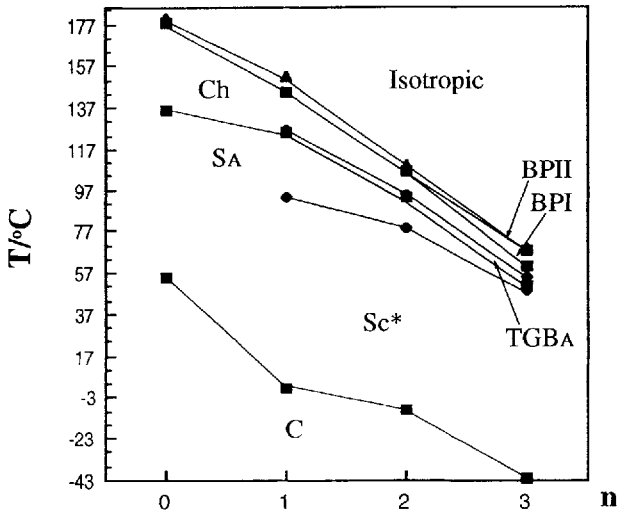

(*a*)

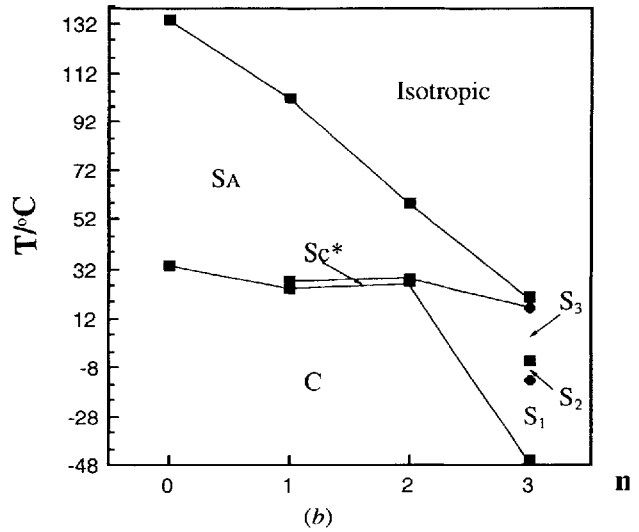

(*b*)

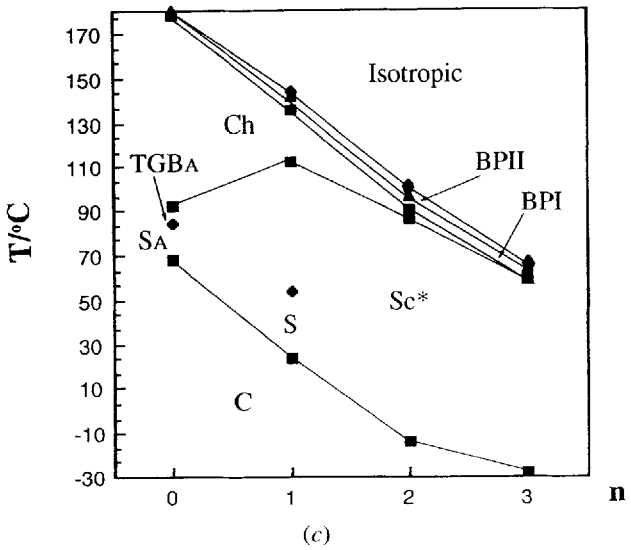

(*c*)

Figure 1. Plots of transition temperatures versus n, the number of oxyethylene spacer chain: (*a*) series MDn12A; (*b*) series MDn12B; (*c*) series MDn12C.

From figure 1 (*a*), the presence of these oxyethylene unit chains significantly depressed the phase transition temperatures. A similar depressing effect of the oxyethylene on the clearing points and crystalline to nematic transition of nematic LCs also has been reported by others [22]. This depression has been attributed to the increased flexibility of these C–O bonds. The temperature ranges of BP, TGB_A and chiral smectic C phases increased as oxyethylene chain unit increased. On the other hand, the temperature ranges of cholesteric and smectic A phases behaved otherwise. It is important to note that this series has a tendency to form the chiral smectic C phase based on the result above.

3.1.3. *Series MDn12B*

This series differed structurally from the MDn12A series. The (*S*)-2-methyl-1-butyl terminal chiral tail of MDn12A was replaced by the (*R*)-1-methylheptyl chiral moiety. The transition temperatures are plotted as a function of units of oxyethylene chain (see figure 1 (*b*)). On cooling from the isotropic liquid, all the compounds exhibited a classical smectic A phase. The chiral smectic C phase was obtained in the homologues with longer spacer chains, $n = 1, 2$. The chiral smectic C phase showed a typical striated fan texture. The homologue with the longest spacer chain, MD312B, exhibited richer smectic polymorphism, S_1, S_2 and S_3. The transition temperatures ($-20°C \sim 40°C$) were too low to be investigated under the microscope, but could be easily detected by calorimetry studies. Compared with MDn12A series and MDn12B series, the longer chiral alkyl chain

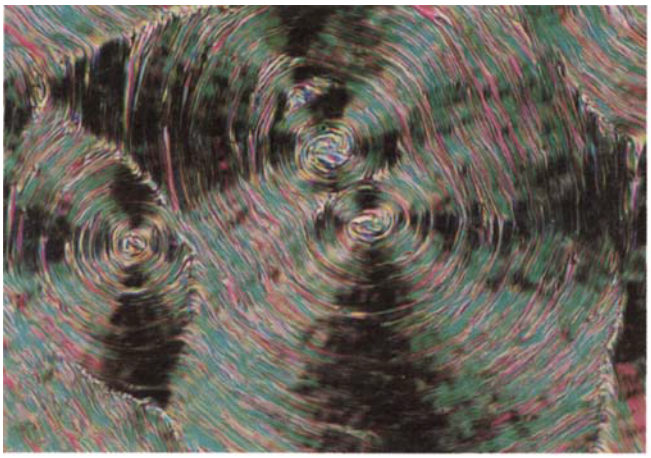

(*a*)

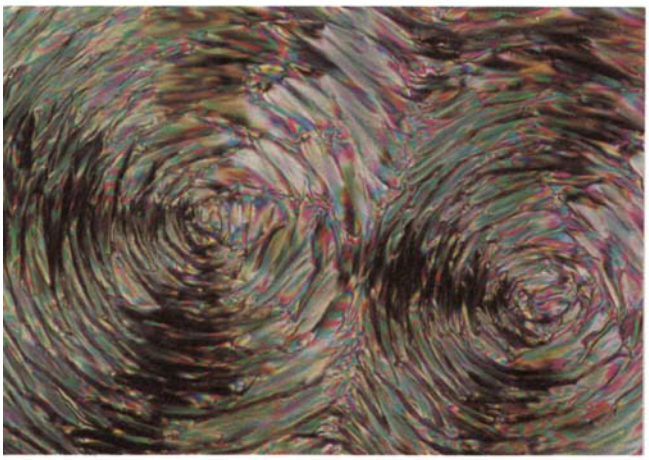

(*b*)

(*c*)

Figure 2. Optical polarizing micrographs displayed by MD312A: (*a*) the filament texture of TGB_A phase at 54·9°C (400 ×); (*b*) spiral smectic A phase at 50·2°C (400 ×); (*c*) chiral smectic C phase at 48·8°C (400 ×).

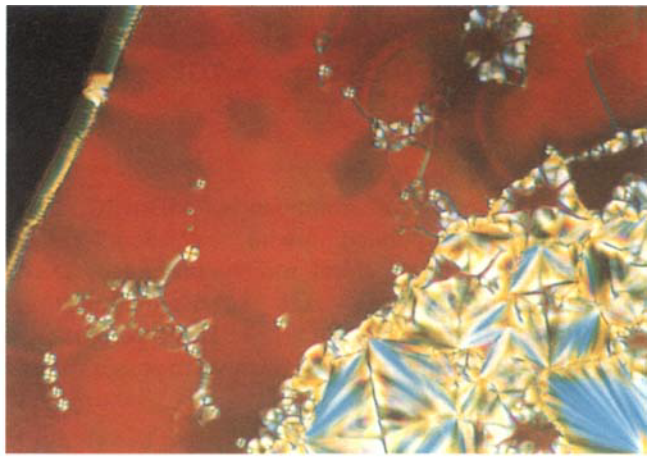

(*a*)

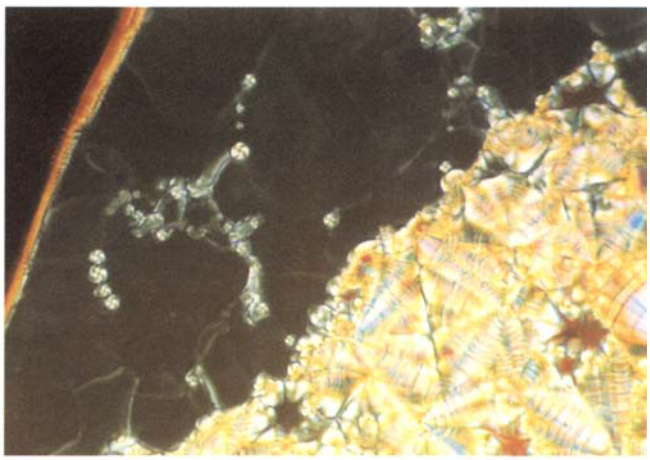

(*b*)

(*c*)

Figure 3. Optical polarizing micrographs displayed by MD212C: (*a*) colourful (orange/red) homeotropic texture at 80·2°C (400 ×); (*b*) dark colour on the same region at 51°C (400 ×); (*c*) chiral smectic C texture on another region at 51°C (400 ×).

(1-methylheptyl) has a stronger tendency to narrow the temperature range of chiral smectic C phase. Similar results have been reported by Waugh *et al.* [23]. Furthermore, no BP, cholesteric or TGB_A phases were observed in the MDn12B series.

3.1.4. *Series MDn12C*

The last series of compounds, MDn12C, were covalently incorporated with (2*S*,3*S*)-2-chloro-3-methylpentanoyloxy chiral moiety instead of (*S*)-2-methyl-1-butoxycarbonyl and (*R*)-1-methylheptoxycarbonyl of MDn12A and MDn12B. This type of moiety with two chiral centres has been reported to possess a large spontaneous polarization [24]. The four compounds of this series were all mesomorphic. Different chiral moieties usually result in different mesophase sequences (see figure 1 (*c*)). MD012C exhibited an I–BPII–BPI–Ch–TGB_A–S_A–C liquid crystal sequence similar to those of compounds MD112A, MD212A and MD312A. However, no chiral smectic C phase was observed for MD012C. MD112C and MD212C exhibited similar liquid crystal behaviour. On cooling from the isotropic, a BP and a cholesteric phase with paramorphosis style were observed. Upon subsequent cooling of the cholesteric phase, the TGB_A phase was not present but a smectic phase with vague striated lines and colourful homeotropic alignment somewhat like the cholesteric texture appeared (see figure 3 (*a*)). It is believed that the phase was not a smectic A phase because it revealed a colourful homeotropic alignment (green/orange colour in MD112C, orange/red colour in MD212C). This is indicative of the existence of a special phase. Further cooling from this special phase, striated lines appeared clearly on the fan domains, and the colourful region started to gradually change into dark colour (see figure 3 (*b*), (*c*)). The initial evaluation of electro-optical properties on MD212C indicated that this phase possessed a chiral smectic C bistability. This result indicated that a ferroelectricity did exist in this phase. For another homologue with longer spacer chain of this series ($n = 3$), MD312C exhibited a BP and chiral smectic C phase with striated lines. No cholesteric phase was observed in MD312C.

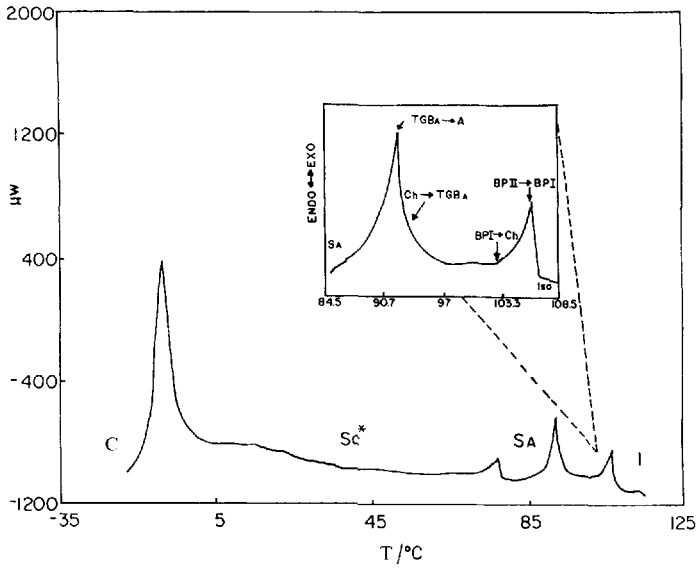

(*a*)

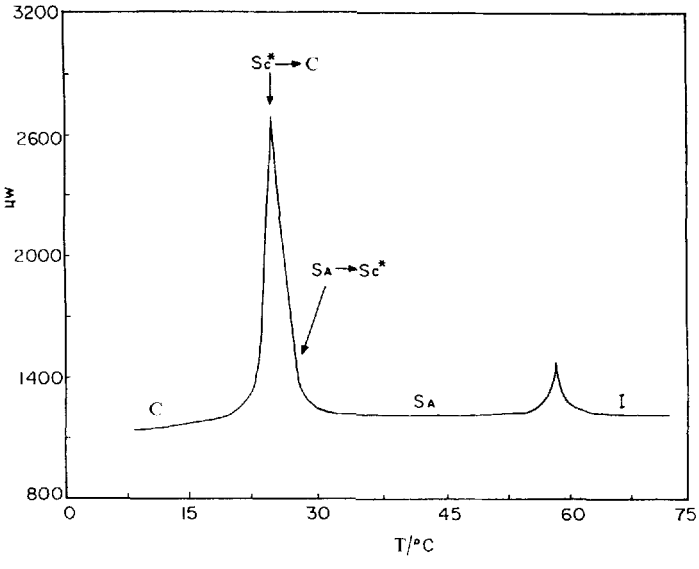

(*b*)

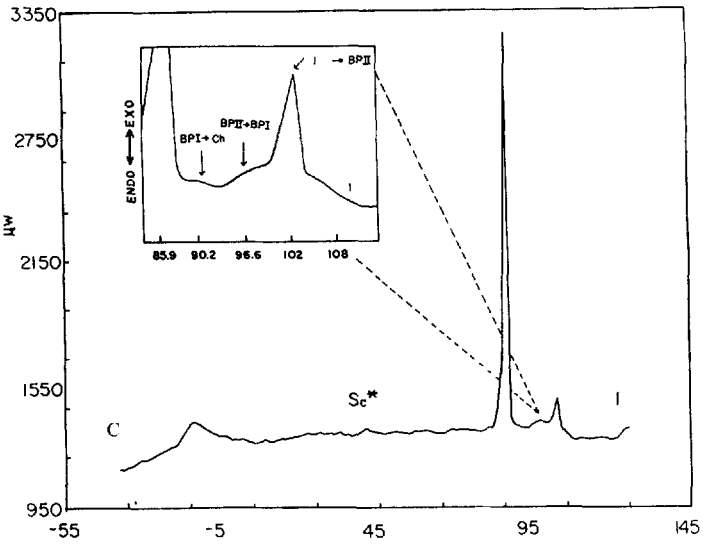

(*c*)

Figure 4. DSC thermograms of (*a*) MD212A (5°C min $^{-1}$, cooling scan), (*b*) MD212B (5°C min $^{-1}$, cooling scan), and (*c*) MD212C (5°C min $^{-1}$, cooling scan).

Table 2. Transition temperatures for racemates (±)MD212A and (±)MD312A.

Name	*n*	Phase transition °C (corresponding enthalpy changes, mJ mg^{-1}) $\left[\frac{\text{Heating}}{\text{Cooling}}\right]$
(±)MD212A	2	$\frac{\text{C } 65{\cdot}6(48{\cdot}8)\,\text{S}_\text{C}\,79{\cdot}2(0{\cdot}5)\,\text{S}_\text{A}\,94{\cdot}6(1{\cdot}2)\,\text{N}\,110{\cdot}7(0{\cdot}7)\,\text{I}}{\text{I}\,108{\cdot}7(0{\cdot}9)\,\text{N}\,92{\cdot}6(1{\cdot}5)\,\text{S}_\text{A}\,76{\cdot}4(0{\cdot}8)\,\text{S}_\text{C}\,-\,9{\cdot}9(20{\cdot}2)\,\text{C}}$
(±)MD312A	3	$\frac{\text{C } 9{\cdot}5(-)\,\text{S}_\text{C}\,46{\cdot}4\,(0{\cdot}6)\,\text{S}_\text{A}\,58{\cdot}5(1{\cdot}1)\,\text{N}\,72{\cdot}2(0{\cdot}6)\,\text{I}}{\text{I}\,72(0{\cdot}7)\,\text{N}\,57{\cdot}2(1{\cdot}1)\,\text{S}_\text{A}\,47{\cdot}4(0{\cdot}7)\,\text{S}_\text{C}\,-\,40{\cdot}9(-)\dagger\,\text{C}}$

† Enthalpies were too small to be evaluated.

The MDn12C series has a significantly narrower smectic A temperature range compared to the MDn12A series compounds with the same spacer length (see figure 1 (*a*) and (*c*)). It is highly irregular that the TGB_A phase was present in the homologue MD012C with such short spacer chain. Normally, the TGB_A phase is only present in liquid crystals with a long spacer chain [18, 21].

3.2. *Calorimetric studies*

Transition enthalpies were determined by differential scanning calorimetry using a Seiko DSC 220C. The transition temperatures and corresponding enthalpies values are given in table 1 (*a*), (*b*). the thermograms were recorded upon cooling at a rate of 5°C min^{-1} (see figure 4 (*a*), (*b*) and (*c*)). For MD112A, MD212A, MD312A and MD012C, it is was very difficult to obtain individual transition enthalpies from the BP/Ch and TGB_A/S_A phases due to overlapping. Only the melting transition enthalpies could be determined unambiguously. The enthalpies of some overlapping phase transitions are given in table 1. Four homologues of series MDn12A underwent a larger degree of supercooling (maximum: 70·9°C for MD212A) than the other three series compounds. This property has been utilized effectively in LC mixtures [9].

3.3. *Racemate studies*

The layered structure of the TGB_A phase was first inferred from studies of racemates of the two compounds (±)MD212A and (±)MD312A. They all exhibited the phase sequence: I–N–S_A–C (see table 2). The smectic A phase was observed instead of TGB_A phase when chirality was eliminated in a racemate. This showed that the TGB_A phase is a variant of the smectic A phase. The temperatures of clarification were higher than those of the optically pure compounds. This result agrees well with the Renn-Lubensky model [25] and the prediction of de Gennes [26].

4. Conclusions

All the novel compounds were liquid crystalline except MD211A and MD311A. The oxyethylene unit as the spacer chain favoured a lowering of the transition temperatures. When the number of oxyethylene units was increased, the transition temperatures decreased. Several compounds ($n = 1, 2, 3$) in the MDn12A series were found to have the phase sequence, Ch–TGB_A–S_A. MD012C of the MDn12C series exhibited the same phase sequence. It was very difficult to obtain enthalpy values for many of the transitions due to overlapping.

The results reported here indicated that the chiral MDn12A series seems to be the right candidate for the formation of a wide temperature range of chiral smectic C (~ 90°C). This phenomenon was also found in the MDn12C series. Therefore they could be very useful for preparing new ferroelectric side chain liquid crystalline polymers (FSCLCPs) with a wide temperature range of chiral smectic C phase, including room temperature.

The MDn12B series had a narrow chiral smectic C temperature range possibly due to longer chiral tail (1-methylheptyl) and oxyethylene spacer chain. For the MDn11A series, the mesophases disappeared in the derivatives with longer spacers ($n = 2, 3$). It can be concluded that oxyethylene chain is more suitable for the formation of the mesophases in three aromatic ring ester system than in two aromatic ring ester system.

5. Experimental

5.1. *Materials*

Allyl bromide, 2-chloroethanol, 2-(2-chloroethoxy)-ethanol, 2-(2-(2-chloroethoxy) ethoxy)ethanol, 4-hydroxy-4′-biphenylcarboxylic acid (from Aldrich); methyl-4-hydroxybenzoate, 4-hydroxybenzoic acid, 4,4′-dihydroxybiphenyl (from TCI); (*S*)-2-methyl-1-butanol (from Fluka); L-2-octanol (from Janssen); L-isoleucine and other reagents (from Merk U.K. Ltd.) were used as received.

5.2. *Measurements*

^{1}H NMR spectra were obtained with a Bruker AM300 MHz spectrometer. All spectra were recorded in $CDCl_3$ with TMS as the internal standard unless otherwise noted. A Seiko DSC 220C differential scanning calorimeter equipped with a 5200H computer system was used to determine the thermal transitions that were read at the maximum of their endothermic or exothermic peaks. In all cases, heating and cooling rates were 5°C min^{-1}, unless otherwise specified. After the first heating scan, the sample was annealed at 10°C above the isotropization temperature for 5–10 min. Under these conditions, beginning with the second heating and cooling scans, all recorded DSC scans gave reproducible data. The transitions reported were read during the second or third heating scan and cooling scan unless otherwise specified. A Nikon Microphot-FX optical polarized microscope equipped with a Mettler FP 82 hot stage and a Mettler FP 80 central processor was used in observing thermal transitions and anisotropic textures.

5.3. *Synthesis*

5.3.1. *(2S, 3S)-2-Chloro-3-methyl-pentanoic acid (1)*

The synthesis of compound (**1**) is according to the method of Koppenhoefer [26]. In a 500 ml, round flask equipped with a magnetic stirrer were placed L-isoleucine (0·2 mol) and 360 ml 5N HCl at 0°C. The cooled sodium nitrite aqueous solution (0·3 mol) was added dropwise under nitrogen below 4°C. After stirring the reaction mixture for 5 h, the ice bath was removed, and the mixture kept at room temperature for 24 h. 16 g calcium carbonate were added, and extracted with ethyl ether. The organic phase was washed with a 10 wt % aqueous solution of HCl, and the solvent evaporated on a rotavapor. The colourless oily product was obtained by vacuum distillation (110°C/8 mmHg, Yield 84·7 per cent). $[\alpha]_d^{25} = -7{\cdot}6$, ^{1}H NMR ($CDCl_3$, TMS): $\delta = 0{\cdot}9$ (t, 3 H, $-CH_2\underline{CH_3}$), 0·97 (d, 3 H, $-CH\underline{CH_3}-C_2H_5-$), 1·27 and 1·58 (m, 2 H, $-\underline{CH_2}CH_3$), 2·03 (m, 1 H, $-\underline{CH}CH_3-$), 4·14 (m, 1 H, $-\underline{CH}Cl-COOH$).

5.3.2. *Methyl 4-(2-hydroxyethoxy)benzoate (2); Methyl 4-(2-(2-hydroxyethoxy)ethoxy)benzoate (3); Methyl 4-(2-(2-(2-hydroxyethoxy)ethoxy)ethoxy) benzoate (4)*

These compounds were synthesized by similar method. An example synthesis of methyl 4-(2-(2-hydroxyethoxy)ethoxy)benzoate (**3**) is presented below: A solution of 2-(2-chloroethoxy)ethanol 5·38 g (0·04 mol) in 50 ml of acetonitrile was added dropwise to a solution of methyl 4-hydroxybenzoate 5·1 g (0·036 mol) and 23·2 g (0·168 mol) of powdered anhydrous potassium carbonate in 300 ml of acetonitrile at 80°C. After stirring the reaction mixture under reflux for 12 h, 250 ml of the acetonitrile was then distilled and 250 ml dichloromethane added. The reaction mixture was filtered through celite and the solid was washed thoroughly with dichloromethane. Evaporation of the filtrate yielded product in the form of a yellow oil. Purification by flash chromatography on silica gel with 40 per cent diethyl ether in dichloromethane yielded 7·1 g (87 per cent). ^{1}H NMR ($CDCl_3$, TMS): $\delta = 2{\cdot}62$ (s, 1 H, $-O\underline{H}$), 3·81–4·25 (m, 8 H, $-(OC\underline{H_2}C\underline{H_2})_2-$), 3·85 (s, 3 H, $-COOC\underline{H_3}$), 6·9 and 7·9 (2d, 4 aromatic protons).

5.3.3. *Methyl 4-allyloxybenzoate (5); Methyl 4-(2-allyloxyethoxy)benzoate (6); Methyl 4-(2-(2-allyloxyethoxy)ethoxy)benzoate (7); Methyl 4-(2-(2-(2-allyloxyethoxy)ethoxy)ethoxy)benzoate (8)*

These compounds were synthesized by the same method. The prepration of methyl 4-(2-(2-allyloxyethoxy)ethoxy)benzoate (**7**) is presented as followed: Methyl 4-(2-(2-hydroxyethoxy)ethoxy)benzoate (**3**) 8·4 g (0·035 mol) was added to a suspension of 3·15 g (0·105 mol) sodium hydride in 100 ml dried tetrahydrofuran at 4°C. After the hydrogen was completely released, allyl bromide 3·94 ml (0·0456 mol) was added dropwise to the reaction mixture and then stirred at room temperature overnight. The excess sodium hydride was treated with distilled water and extracted with ethyl acetate. The organic phase was washed with 10 per cent aqueous hydrochloric acid solution, dried over anhydrous $MgSO_4$, and the solvent evaporated on a rotary evaporator. The yellow oil product was purified by flash chromatography on silica gel with 4 per cent diethyl ether in dichloromethane. Yield 8·39 g (86 per cent). ^{1}H NMR ($CDCl_3$, TMS): $\delta = 3{\cdot}81$–4·25 (m, 10 H, $-CH_2-(OC\underline{H_2}C\underline{H_2})_2-$), 3·85 (s, 3 H, $-COOC\underline{H_3}$), 5·23 and 5·9 (m, 3 H, $C\underline{H_2}=C\underline{H}-$), 6·95 and 8·05 (2d, 4 aromatic protons).

5.3.4. *4-Allyloxybenzoic acid (9); 4-(2-Allyloxyethoxy)benzoic acid (10); 4-(2-(2-Allyloxyethoxy)ethoxy)benzoic acid (11); 4-(2-(2-(2-Allyloxyethoxy)ethoxy)ethoxy)benzoic acid (12)*

These compounds were synthesized by similar method. An example synthesis of 4-(2-(2-allyloxyethoxy)-ethoxy)benzoic acid (**11**) is presented below: A mixture of 8·39 g (0·03 mol) of methyl 4-(2-(2-allyloxyethoxy)-ethoxy) benzoate (**7**), 6 ml of 50 per cent aqueous sodium hydroxide solution and 150 ml of methanol was stirred under reflux for 3 h. Methanol was distilled off (100 ml) and water 600 ml was added. The reaction mixture was acidified with hydrochloric acid. After cooling at 0°C, a white solid was filtered and set aside. The filtrate was extracted with dichloromethane and the extracted material was evaporated to a white solid which was combined with the set-aside material. The combined material was dried

Table 3. (*a*) Chemical shift δ and $[\alpha]_d^{25}$ value of series MDn11A, MDn12A.

Monomers	$[\alpha]_d^{25}$†	^{1}H NMR spectra‡
MD011A	+ 2·94	1·0 (m, 6H, –CHC<u>H</u>$_3$–CH$_2$C<u>H</u>$_3$), 1·3 and 1·5 (m, 2H, –C<u>H</u>$_2$CH$_3$), 1·8 (m, 1H, –C<u>H</u>CH$_3$), 4·2 and 4·3 (m, 2H, –O–C<u>H</u>$_2$–), 4·6 (m, 2H, –C<u>H</u>$_2$–O–), 5·23 and 5·9 (m, 3H, C<u>H</u>$_2$=C<u>H</u>–), 6·9–7·9 (4d, 8 aromatic protons).
MD111A	+ 2·66	1·0 (m, 6H, –CHC<u>H</u>$_3$–CH$_2$C<u>H</u>$_3$), 1·3 and 1·5 (m, 2H, –C<u>H</u>$_2$CH$_3$), 1·8 (m, 1H, –C<u>H</u>CH$_3$), 4·2 and 4·3 (m, 2H, –O–C<u>H</u>$_2$–), 3·81–4·25 (m, 6H, –C<u>H</u>$_2$–(OC<u>H</u>$_2$C<u>H</u>$_2$)–), 5·23 and 5·9 (m, 3H, C<u>H</u>$_2$=CH–), 6·9–7·9 (4d, 8 aromatic protons).
MD211A	+ 1·98	1·0 (m, 6H, –CHC<u>H</u>$_3$–CH$_2$C<u>H</u>$_3$), 1·3 and 1·5 (m, 2H, –C<u>H</u>$_2$CH$_3$), 1·8 (m, 1H, –C<u>H</u>CH$_3$), 4·2 and 4·3 (m, 2H, –O–C<u>H</u>$_2$–), 3·81–4·25 (m, 10H, –C<u>H</u>$_2$–(OC<u>H</u>$_2$C<u>H</u>$_2$)$_2$–), 5·23 and 5·9 (m, 3H, C<u>H</u>$_2$=CH–), 6·9–7·9 (4d, 8 aromatic protons).
MD311A	+ 1·567	1·0 (m, 6H, –CHC<u>H</u>$_3$–CH$_2$C<u>H</u>$_3$), 1·3 and 1·5 (m, 2H, –C<u>H</u>$_2$CH$_3$), 1·8 (m, 1H, –C<u>H</u>CH$_3$), 4·2 and 4·3 (m, 2H, –O–C<u>H</u>$_2$–), 3·81–4·25 (m, 14H, –C<u>H</u>$_2$–(OC<u>H</u>$_2$C<u>H</u>$_2$)$_3$–), 5·23 and 5·9 (m, 3H, C<u>H</u>$_2$=CH–), 6·9–7·9 (4d, 8 aromatic protons).
MD012A	+ 2·57	1·0 (m, 6H, –CHC<u>H</u>$_3$–CH$_2$C<u>H</u>$_3$), 1·3 and 1·5 (m, 2H, –C<u>H</u>$_2$CH$_3$), 1·8 (m, 1H, –C<u>H</u>CH$_3$), 4·2 and 4·3 (m, 2H, –O–C<u>H</u>$_2$–), 4·6 (m, 2H, –C<u>H</u>$_2$–O–), 5·23 and 5·9 (m, 3H, C<u>H</u>$_2$=C<u>H</u>–), 6·9–8·0 (6d, 12 aromatic protons).
MD112A	+ 2·203	1·0 (m, 6H, –CHC<u>H</u>$_3$–CH$_2$C<u>H</u>$_3$), 1·3 and 1·5 (m, 2H, –C<u>H</u>$_2$CH$_3$), 1·8 (m, 1H, –C<u>H</u>CH$_3$), 4·2 and 4·3 (m, 2H, –O–C<u>H</u>$_2$–), 3·81–4·25 (m, 6H, –C<u>H</u>$_2$–(OC<u>H</u>$_2$C<u>H</u>$_2$)–), 5·23 and 5·9 (m, 3H, C<u>H</u>$_2$=CH–), 6·9–8·05 (6d, 12 aromatic protons).
MD212A	+ 1·513	1·0 (m, 6H, –CHC<u>H</u>$_3$–CH$_2$C<u>H</u>$_3$), 1·3 and 1·5 (m, 2H, –C<u>H</u>$_2$CH$_3$), 1·8 (m, 1H, –C<u>H</u>CH$_3$), 4·2 and 4·3 (m, 2H, –O–C<u>H</u>$_2$–), 3·81–4·25 (m, 10H, –C<u>H</u>$_2$–(OC<u>H</u>$_2$C<u>H</u>$_2$)$_2$–), 5·23 and 5·9 (m, 3H, C<u>H</u>$_2$=CH–), 6·9–8·05 (6d, 12 aromatic protons).
MD312A	+ 1·463	1·0 (m, 6H, –CHC<u>H</u>$_3$–CH$_2$C<u>H</u>$_3$), 1·3 and 1·5 (m, 2H, –C<u>H</u>$_2$CH$_3$), 1·8 (m, 1H, –C<u>H</u>CH$_3$), 4·2 and 4·3 (m, 2H, –O–C<u>H</u>$_2$–), 3·81–4·25 (m, 14H, –C<u>H</u>$_2$–(OC<u>H</u>$_2$C<u>H</u>$_2$)$_3$–), 5·23 and 5·9 (m, 3H, C<u>H</u>$_2$=CH–), 6·9–8·05 (6d, 12 aromatic protons).

† These values were measured in $CHCl_3$, 25°C.

‡ These values were measured in $CDCl_3$, using 300 MHz nuclear magnetic resonance spectroscopy (internal standard tetramethylsilane).

under vacuum to yield 4·4 g of product (94·3 per cent). ^{1}H NMR ($CDCl_3$, TMS): δ = 3·81–4·25 (m, 10H, –C<u>H</u>$_2$–(OC<u>H</u>$_2$C<u>H</u>$_2$)$_2$–), 5·23 and 5·9 (m, 3H, C<u>H</u>$_2$=C<u>H</u>–), 6·95 and 8·05 (2d, 4 aromatic protons), 12·2 (s, 1H, –COO<u>H</u>).

5.3.5. *(S)-2-Methyl-1-butyl 4-hydroxybenzoate (**13**); 4-4'-Dihydrobiphenyl (2S,3S)-2-chloro-3-methyl pentanoate (**16**)*

The two compounds could be prepared from 4-hydroxybenzoic acid, 4-4'-biphenyl and (*S*)-2-methyl-1-butanol, (2*S*,3*S*)-2-chloro-3-methyl pentanoic acid (**1**) via a esterification. An example synthesis of compound (**13**): In a 250 ml round-bottomed flask, 4-hydroxybenzoic acid 4·14 g (0·03 mol), (*S*)-2-methyl-1-butanol 4·3 ml (0·04 mol), DCC (dicyclohexyl-carbodiimide) 6·18 g (0·03 mol), 4-pyrrolidino pyridine 0·444 g (0·003 mol) and dried THF 50 ml were stirred under N_2 at 4°C overnight. The solution was filtered and filtrate was washed with 10 per cent HCl(aq) and 5 per cent $NaHCO_3$(aq). The filtrate was evaporated to a crudely yellow oil. The product was purified by flash chromatography on silica gel with 40 per cent diethyl ether in dichloromethane. Yield: (**13**) 70·5 per cent; (**16**) 79·36 per cent. m.p.: (**13**) < 25°C, (**16**) 121°C. ^{1}H NMR ($CDCl_3$, TMS): (**13**) 1·0 (m, 6H, –CHC<u>H</u>$_3$–CH$_2$C<u>H</u>$_3$), 1·3 and 1·5 (m, 2H, –C<u>H</u>$_2$CH$_3$), 1·8 (m, 1H, –C<u>H</u>CH$_3$), 4·2 and 4·3 (m, 2H, –O–C<u>H</u>$_2$–), 7·0 and 8·0 (2d, 4H, aromatic protons). (**16**) 0·9 (t, 3H, –CH$_2$C<u>H</u>$_3$), 0·97 (d, 3H, –CHC<u>H</u>$_3$–C$_2$H$_5$), 1·27 and 1·58 (m, 2H, –C<u>H</u>$_2$CH$_3$), 2·03 (m, 1H, –C<u>H</u>CH$_3$), 4·14 (m, 1H, –C<u>H</u>Cl–COO), 6·9, 7·5, 7·6 and 8·05 (4d, 8H, aromatic protons).

Table 3. (*b*) Chemical shift δ and $[\alpha]_d^{25}$ value of series MDn12B, MDn12C.

Monomers	$[\alpha]_d^{25}$†	^{1}H NMR spectra‡
MD012B	+ 26·744	0·9 (t, 3 H, –$(CH_2)_4$–$C\underline{H}_3$), 1·34 (d, 3 H, –OCH ($C\underline{H}_3$)–), 1·26–2·28 (m, 10 H, –$(C\underline{H}_2)_5$–CH_3), 4·44 (m, 1 H, –O–$C\underline{H}(CH_3)$–CH_2–), 4·6 (m, 2 H, –$C\underline{H}_2$–O–), 5·23 and 5·9 (m, 3 H, $C\underline{H}_2$=$C\underline{H}$–), 6·9–8·05 (6d, 12 aromatic protons).
MD112B	+ 25·92	0·9 (t, 3 H, –$(CH_2)_4$–$C\underline{H}_3$), 1·34 (d, 3 H, –OCH ($C\underline{H}_3$)–), 1·26–2·28 (m, 10 H, –$(C\underline{H}_2)_5$–CH_3), 4·44 (m, 1 H, –O–$C\underline{H}(CH_3)$–CH_2–), 3·81–4·25 (m, 6 H, –$C\underline{H}_2$–$(OC\underline{H}_2C\underline{H}_2)$–), 5·23 and 5·9 (m, 3 H, $C\underline{H}_2$=$C\underline{H}$–), 6·9–8·05 (6d, 12 aromatic protons).
MD212B	+ 23·28	0·9 (t, 3 H, –$(CH_2)_4$–$C\underline{H}_3$), 1·34 (d, 3 H, –OCH ($C\underline{H}_3$)–), 1·26–2·28 (m, 10 H, –$(C\underline{H}_2)_5$–CH_3), 4·44 (m, 1 H, –O–$C\underline{H}(CH_3)$–CH_2–), 3·81–4·25 (m, 10 H, –$C\underline{H}_2$–$(OC\underline{H}_2C\underline{H}_2)_2$–), 5·23 and 5·9 (m, 3 H, $C\underline{H}_2$=$C\underline{H}$–), 6·9–8·05 (6d, 12 aromatic protons).
MD312B	+ 21·599	0·9 (t, 3 H, –$(CH_2)_4$–$C\underline{H}_3$), 1·34 (d, 3 H, –OCH ($C\underline{H}_3$)–), 1·26–2·28 (m, 10 H, –$(C\underline{H}_2)_5$–CH_3), 4·44 (m, 1 H, –O–$C\underline{H}(CH_3)$–CH_2–), 3·81–4·25 (m, 14 H, –$C\underline{H}_2$–$(OC\underline{H}_2C\underline{H}_2)_3$–), 5·23 and 5·9 (m, 3 H, $C\underline{H}_2$=$C\underline{H}$–), 6·9–8·05 (6d, 12 aromatic protons).
MD012C	− 3·012	0·9 (t, 3 H, –$CH_2C\underline{H}_3$), 0·97 (d, 3 H, –$CHC\underline{H}_3$–C_2H_5), 1·27 and 1·58 (m, 2 H, –$C\underline{H}_2CH_3$), 2·03 (m, 1 H, –$C\underline{H}CH_3$), 4·14 (m, 1 H, –$C\underline{H}$Cl–COO), 4·6 (m, 2 H, –$C\underline{H}_2$–O–), 5·23 and 5·9 (m, 3 H, $C\underline{H}_2$=$C\underline{H}$–), 6·9–8·05 (6d, 12 aromatic protons).
MD112C	− 3·423	0·9 (t, 3 H, –$CH_2C\underline{H}_3$), 0·97 (d, 3 H, –$CHC\underline{H}_3$–C_2H_5), 1·27 and 1·58 (m, 2 H, –$C\underline{H}_2CH_3$), 2·03 (m, 1 H, –$C\underline{H}CH_3$), 4·14 (m, 1 H, –$C\underline{H}$Cl–COO), 3·81–4·25 (m, 6 H, –$C\underline{H}_2$–$(OC\underline{H}_2C\underline{H}_2)$–), 5·23 and 5·9 (m, 3 H, $C\underline{H}_2$=$C\underline{H}$–), 6·9–8·05 (6d, 12 aromatic protons).
MD212C	− 7·523	0·9 (t, 3 H, –$CH_2C\underline{H}_3$), 0·97 (d, 3 H, –$CHC\underline{H}_3$–C_2H_5), 1·27 and 1·58 (m, 2 H, –$C\underline{H}_2CH_3$), 2·03 (m, 1 H, –$C\underline{H}CH_3$), 4·14 (m, 1 H, –$C\underline{H}$Cl–COO), 3·81–4·25 (m, 10 H, –$C\underline{H}_2$–$(OC\underline{H}_2C\underline{H}_2)_2$–), 5·23 and 5·9 (m, 3 H, $C\underline{H}_2$=$C\underline{H}$–), 6·9–8·05 (6d, 12 aromatic protons).
MD312C	− 5·889	0·9 (t, 3 H, –$CH_2C\underline{H}_3$), 0·97 (d, 3 H, –$CHC\underline{H}_3$–C_2H_5), 1·27 and 1·58 (m, 2 H, –$C\underline{H}_2CH_3$), 2·03 (m, 1 H, –$C\underline{H}CH_3$), 4·14 (m, 1 H, –$C\underline{H}$Cl–COO), 3·81–4·25 (m, 14 H, –$C\underline{H}_2$–$(OC\underline{H}_2C\underline{H}_2)_3$–), 5·23 and 5·9 (m, 3 H, $C\underline{H}_2$=$C\underline{H}$–), 6·9–8·05 (6d, 12 aromatic protons).

† These values were measured in $CHCl_3$, 25°C.

‡ These values were measured in $CDCl_3$, using 300 MHz nuclear magnetic resonance spectroscopy (internal standard tetramethylsilane).

5.3.6. *(S)-2-Methyl-1-butyl 4-hydroxybiphenyl-4'-carboxylate* (**14**); *(R)-1-Methyl-1-heptyl 4-hydroxybiphenyl-4'-carboxylate* (**15**)

Mitsunobu [28] reaction can be used to prepare compound (**14**) and (**15**). An example synthesis of compound (**14**) is presented below: A solution of (*S*)-2-methyl-1-butanol 1·505 ml (0·014 mol) and TPP (triphenylphosphine) 2·447 grams (0·009 mol) in 20 ml of dried THF was added dropwise to a solution of 4-hydroxybiphenyl-4'-carboxylic acid 2 g (0·009 mol) and 23·2 g (0·168 mol) of DEAD (diethyl azodicarboxylate) 1·625 g (0·009 mol) in 20 ml of dried THF at room temperature. After stirring the reaction mixture under reflux for 24 h, the reaction mixture was filtered through celite. Evaporation of the filtrate yielded the product in the form of a yellow oil. Purification by flash chromatography on silica gel with 40 per cent diethyl ether in dichloromethane yielded 2·12 g (80 per cent) m.p.: (**14**) 104°C, (**15**) 111·8°C. ^{1}H NMR ($CDCl_3$, TMS): (**14**) 1·0 (m, 6 H, –$CHC\underline{H}_3$–$CH_2C\underline{H}_3$), 1·3 and 1·5 (m, 2 H, –$C\underline{H}_2CH_3$), 1·8 (m, 1 H, –$C\underline{H}CH_3$), 4·2 and 4·3 (m, 2 H, –O–$C\underline{H}_2$–), 6·9, 7·5, 7·6 and 8·05 (4d, 8 H, aromatic protons). (**15**) 0·9 (t, 3 H, –$(CH_2)_4$–$C\underline{H}_3$), 1·34 (d, 3 H, –OCHC$\underline{H}_3$–), 1·26–2·28 (m, 10 H, –$(C\underline{H}_2)_5$–CH_3), 4·44 (m, 1 H, –O–$C\underline{H}CH_3$–CH_2–), 6·9, 7·5, 7·6 and 8·05 (4d, 8 H, aromatic protons).

5.3.7. *MDn11A*

4-[(*S*)-2-Methyl-1-butoxycarbonyl]phenyl 4-allyloxybenzoate (**17**); 4-[(*S*)-2-Methyl-1-butoxycarbonyl]phenyl

4-(2-alloyloxyethoxy)benzoate (**18**); 4-[(*S*)-2-Methyl-1-butoxycarbonyl]phenyl 4-(2-(2-allyloxyethoxy)ethoxy) benzoate (**19**); 4-[(*S*)-2-Methyl-1-butoxycarbonyl]phenyl 4-(2-(2-(2-allyloxyethoxy)ethoxy)ethoxy)benzoate (**20**);.

5.3.8. *MDn12A*

4-[(*S*)-2-Methyl-1-butoxycarbonyl]-4′-biphenyl 4-allyloxy benzoate (**21**); 4-[(*S*)-2-Methyl-1-butoxycarbonyl]-4′-biphenyl 4-(2-allyloxyethoxy)benzoate (**22**); 4-[(*S*)-2-Methyl-1-butoxycarbonyl]-4′-biphenyl 4-(2-(2-allyloxyethoxy)ethoxy)benzoate (**23**); 4-[(*S*)-2-Methyl-1-butoxycarbonyl]-4′-biphenyl 4-(2-(2-(2-allyloxyethoxy)-ethoxy)ethoxy)benzoate (**24**).

5.3.9. *MDn12B*

4-[(*R*)-1-Methyl-1-heptoxycarbonyl]-4′-biphenyl 4-allyloxybenzoate (**25**); 4-[(*R*)-1-Methyl-1-heptoxycarbonyl]-4′-biphenyl 4-(2-allyloxyethoxy)benzoate (**26**); 4-[(*R*)-1-Methyl-1-heptoxycarbonyl]-4′-biphenyl 4-(2-(2-allyloxyethoxy)ethoxy)benzoate (**27**); 4-[(*R*)-1-Methyl-1-heptoxycarbonyl]-4′-biphenyl 4-(2-(2-(2-allyloxyethoxy)ethoxy)ethoxy)benzoate (**28**).

5.3.10. *MDn12C*

4-[(2*S*, 3*S*)-2-Chloro-3-methylpentanoyloxy]-4′-biphenyl 4-allyloxybenzoate (**29**); 4-[(2*S*, 3*S*)-2-Chloro-3-methylpentanoyloxy]-4′-biphenyl 4-(2-allyloxyethoxy)benzoate (**30**); 4-[(2*S*, 3*S*)-2-Chloro-3-methyl-pentanoyloxy]-4′-biphenyl 4-(2-(2-allyloxyethoxy)ethoxy)benzoate (**31**); 4-[(2*S*, 3*S*)-2-Chloro-3-methyl-pentanoyloxy]-4′-biphenyl 4-(2-(2-(2-allyloxyethoxy)ethoxy)ethoxy)benzoate (**32**).

These final products were synthesized by the same method of preparing compounds (**13**), (**16**), or compounds (**14**), (**15**). The $[\alpha]_d^{25}$, ^{1}H NMR spectra are listed in table 3 (*a*), (*b*).

The authors are grateful to the National Science Council of the Republic of China (NSC-81-0416-E007-02 and NSC-82-0511-E007-01).

References

[1] Meyer, R. B., Liebert, L., Strzelecki, L., and Keller, J. P., 1975, *J. Phys. Lett., Paris*, **36,** 69.
[2] Clark, N. A., and Largerwall, S. T., 1980, *Appl. Phys. Lett.*, **36,** 898.
[3] Leslie, T. M., 1984, *Ferroelectrics*, **58,** 9.
[4] Furakawa, K., Terashima, K., Ichihashi, M., Inoue, H., Saito, S., and Inukai, T., 1985, *6th Liq. Cryst. Conf. Soc. Count.*, Halle (GDR), Abstract, A37.
[5] Furakawa, K., and Terashima, K., 1986, Eur. Pat., Appl., EP 178 647.
[6] Keller, P., 1984, *Molec. Crystals liq. Crystals*, **102,** 295.
[7] Koden, M., Katsuse, H., Itoh, N., Kaneko, T., Tamai, K., Takeda, H., Shiomi, M., Numao, N., Kido, M., Matsuki, M., Miyoshi, S., and Wada, T., 1993, *Abstracts of Fourth International Conference on Ferroelectric Liquid Crystals*, p-146, p. 369.
[8] Tajima, E., Kondoh, S., and Suzuki, Y., 1993, *Abstracts of Fourth International Conference on Ferroelectric Liquid Crystals*, p-147, p. 371.
[9] Adams, T. G., and Sinta, R., 1989, *Molec. Crystals liq. Crystals*, **177,** 145.
[10] Scherowsky, G., Schliwa, A., Springer, J., Kuhnpast, K., and Trapp, W., 1989, *Liq. Crystals*, **5,** 1281.
[11] Shibaev, V. P., Kozlovsky, M. V., and Plate, N. A., 1990, *Liq. Crystals*, **8,** 1281.
[12] Vallerien, S. U., Kremer, F., and Fischer, E. W., 1990, *Makromolek. Chem. rap. Commun.*, **11,** 593.
[13] Kapizta, H., and Zentel, R., 1991, *Makromolek. Chem.*, **192,** 1859.
[14] Hsiue, G. H., Hsu, C. H., and Shin, L. J., 1993, *Makromolecules*, **26,** 3161.
[15] Wu, S. L., Hsieh, W. J., Chen, D. G., Chen, S. J., Shy, J. T., and Hsiue, G. H., 1994, *Molec. Crystals liq. Crystals* (in the press).
[16] Chen, J. H., Chang, R. C., and Hsiue, G. H., 1993, *Ferrolectrics*, **147,** 241.
[17] Goodby, J. W., Waugh, M. A., Stein, S. M., Chin, E., Pindak, R., and Patel, J. S., 1989, *Nature, Lond.*, **337,** 449.
[18] Goodby, J. W., Waugh, M. A., Stein, S. M., Chin, E., Pindak, R., and Patel, J. S., 1989, *J. Am. chem. Soc.*, **111,** 8119.
[19] Slaney, A. T., and Goodby, J. W., 1991, *J. mater. Chem.*, **1,** 5.
[20] Slaney, A. T., and Goodby, J. W., 1991, *Liq. Crystals*, **9,** 849.
[21] Nguyen, H. T., Twieg, R. T., Nabor, M. F., Isaert, N., and Destrade, C., 1991, *Ferroelectrics*, **121,** 187.
[22] Kitamura, T., Fujii, T., and Mukoh, A., 1984, *Molec. Crystals liq. Crystals*, **108,** 333.
[23] Waugh, M. A., Stein, S. M., Chin, E., and Goodby, J. W., 1992, *Liq. Crystals*, **11,** 135.
[24] Dumon, M., Nguyen, H. T., Mauzac, M., Destrade, C., Achard, M. F., and Gasparoux, H., 1990, *Macromolecules*, **23,** 357.
[25] Renn, S. R., and Lubensky, T. C., 1991, *Molec. Crystals liq. Crystals*, **209,** 349.
[26] De Gennes, P. G., 1972, *Solid St. Commun.*, **10,** 753.
[27] Koppenhoefer, B., and Schurig, V., 1987, *J. org. Synth.*, **66,** 151.
[28] Mitsunobu, O., 1981, *Synthesis*, p. 1.